**Revista de Metalurgia** 56(4)
October–December 2020, e179
ISSN-L: 0034-8570
https://doi.org/10.3989/revmetalm.179

# Low cycle fatigue behavior of Platinum-Aluminide coated Rene®80 near and above the DBTT

Mohammad Mehdi Barjesteh[a,✉], Seyed Mehdi Abbasi[a],
Karim Zangeneh Madar[a], Kourosh Shirvani[b]

[a]Faculty of Material and Manufacturing Technologies, Malek Ashtar University of Technology (MUT), Babaie street, Lavizan, 15875-1774, Tehran, Iran

[b]Department of Advanced Materials and New Energies, Iranian Research organization for Science and Technology (IROST), 33535-111, Tehran, Iran

(✉Corresponding author: mmbarjesteh@yahoo.com)

Submitted: 23 May 2020; Accepted: 9 October 2020; Available On-line: 11 January 2020

**ABSTRACT:** Ni-based superalloy Rene®80 is used for manufacturing gas turbine blades in jet engines. The life-time of some jet engine turbine blades is limited by low cycle fatigue and this property has been strongly affected by coatings. *Ductile to Brittle Transition Temperature* (DBTT) is the most important factor which affects the mechanical properties of coated alloys. In this study, high temperature-low cycle fatigue behavior of uncoated and coated Rene®80 by platinum-aluminide (Pt-Al) was evaluated at temperatures 871 °C (near the DBTT) and 982 °C (above the DBTT). Results of low cycle fatigue tests under strain-controlled condition at 871 °C for $R$ =0 and strain rate of $2\times10^{-3}$ $s^{-1}$, at a total strain range of 0.8% showed a decrease in fatigue strength of coated specimens about 14%, compared to the uncoated ones. However, increasing the testing temperature from 871 °C to 982 °C, led to an increase in the low cycle fatigue behavior of coated Rene®80 about 10% as compared to the uncoated specimens.

**KEYWORDS:** DBTT; Fractography; Low cycle fatigue; Platinum-aluminide; Rene®80

**Citation/Citar como:** Barjesteh, M.M.; Abbasi, S.M.; Zangeneh Madar, K.; Shirvani, K. (2020). "Low cycle fatigue behavior of Platinum-Aluminide coated Rene®80 near and above the DBTT". *Rev. Metal.* 56(4): e179. https://doi.org/10.3989/revmetalm.179

**RESUMEN:** *Comportamiento a fatiga de baja frecuencia del compuesto Rene®80 recubierto de aluminuro de platino cerca y por encima del DBTT*. La superaleación Rene®80 a base de Ni se utiliza para fabricar álabes de turbinas de gas en motores a reacción. La vida útil de algunas palas de turbina de motores a reacción está limitada por la fatiga de baja frecuencia y esta propiedad se ha visto fuertemente afectada por los revestimientos. La temperatura de transición de dúctil a frágil (DBTT) es el factor más importante que afecta las propiedades mecánicas de las aleaciones recubiertas. En este estudio, se evaluó el comportamiento de fatiga a alta temperatura y baja frecuencia del compuesto Rene®80 sin recubrimiento y recubierto con aluminuro de platino (Pt-Al) a temperaturas de 871 °C (cerca del DBTT) y 982 °C (por encima del DBTT). Los resultados de las pruebas de fatiga, en condiciones de deformación controlada a 871 °C para R = 0 y una tasa de deformación de $2\times10^{-3}$ $s^{-1}$, en un intervalo de deformación total de 0,8%, mostraron una disminución de la resistencia a la fatiga de las muestras recubiertas de aproximadamente un 14%, en comparación con las no recubiertas. Sin embargo, el aumento de la temperatura de prueba de 871 °C a 982 °C, condujo a un aumento en el comportamiento a fatiga de baja frecuencia del compuesto Rene®80 recubierto en aproximadamente un 10% en comparación con las muestras sin recubrir.

**PALABRAS CLAVE:** Aluminuro de platino; DBTT; Fatiga a baja frecuencia; Fractografía; Rene®80

**ORCID ID:** Mohammad Mehdi Barjesteh (https://orcid.org/0000-0001-7461-9007); Seyed Mehdi Abbasi (https://orcid.org/0000-0003-3355-7318); Karim Zangeneh Madar (https://orcid.org/0000-0002-2645-3468); Kourosh Shirvani (https://orcid.org/0000-0002-2462-8885)

## 1. INTRODUCTION

Rene®80 (General Electric trademark) is a cast nickel-based superalloy used for manufacturing of first stage turbine blades of jet engines. This superalloy is generally used at the temperature range of 760–982 °C (Safari and Nategh, 2006). Protective coatings are deposited on the surface of airfoil turbine blades, in order to enhance the corrosion and oxidation resistance of the base alloys at high temperatures. It has been known that the formation of a protective alumina scale based on intermetallic β-NiAl compound, improves the oxidation resistance of the base alloys (Rahmani and Nategh, 2008a). More improvement in cyclic oxidation and hot corrosion resistance of superalloys has been reported by controlling the addition of precious metals such as platinum to β-NiAl compound (Krishna *et al.*, 1998). Although the presence of Pt in aluminide coatings causes an improvement in their cyclic oxidation resistance at high temperatures, a minimum content of Pt (corresponding to a 6 mm thick initial Pt layer) in the coating is necessary in order to realize its beneficial effects fully (Krishna *et al.*, 1998). To produce the platinum-aluminide (Pt-Al) coating, an initial layer of platinum was applied on the considered surface and after that, aluminum is diffused into it. In the diffusion coatings, the differences in the composition of the coating and substrate, as a result of coating and the substrate element combinations, have a significant effect on the mechanical properties of the alloy. (Ni, Pt)Al and $PtAl_2$ phases which are formed during Pt-Al coating process, are inherently brittle and during service, are prone to cracking at low temperature. The DBTT (*Ductile to Brittle Transition Temperature*) of aluminide bond coats by micro-tensile test method was evaluated in a study Alam *et al.* (2010), They found that the Pt-Al coating has a higher DBTT than a plain aluminide coating. The DBTT values for various Pt-Al and plain aluminide coatings have been reported in the range of 850–1000 and 700–800 °C, respectively. The contents of Al and Pt in Pt-Al coatings have a significant effect on DBTT. It means that coatings with higher surface aluminum and platinum levels exhibited a higher DBTT. The formation of a continuous layer of $PtAl_2$ on the surface of Pt-Al coatings, is a reason for this phenomenon (Vogel *et al.*, 1987). Depending on working temperature, below or above DBTT, negative or positive effects of the coating on mechanical properties of the base alloys are reported. The DBTT is the temperature at which the slope of the strain-temperature curve changes significantly. This temperature is affected by coating process, phase distribution, composition, heat treatment and microstructure. Diffusion coatings exhibit low ductility below the DBTT, whereas above this temperature ductility increases (Bose, 2007). Decreased low cycle fatigue (LCF) properties of Rene®80 alloy following the application of CODEP-B, a plain aluminide coating, at the total strain range 1.2%, and an increase in this property at total strains below 0.8% at 871 °C have been reported by Rahmani and Nategh (2008b), while applying of Pt-Al coating on this superalloy reduced low cycle fatigue property at the same total strain and temperature conditions (Barjesteh *et al.*, 2019a).

Since fatigue failures are in most cases initiated at the surface, in the absence of internal defects and porosity, a coating may potentially affect fatigue strength of coated components, therefore, to study the influence of coating on the fatigue of superalloy has important significance. Nowadays, designers of jet engines, increase the turbine inlet temperature (TIT) with the aim of improving the performance of jet engines. As a result, the fatigue behavior of coated rotary components, such as turbine blades, has been affected by temperature variations. In the present study, the effect of temperature (near and above the DBTT) on low cycle fatigue of a high activity Pt-Al coated Rene®80 was evaluated.

## 2. MATERIALS AND METHODS

The cast nickel base superalloy Rene®80 (nominal composition: 0.16 C, 13.81 Cr, 9.69 Co, 4.23 Mo, 4.02 W, 3.02 Al, 4.87 Ti, 0.12 Fe, 0.05 Zr, 0.05 V, 0.03 Mn, 0.02 B, 0.02 Si, balance Ni, in wt.%, as determined by quantometer apparatus) was used as the substrate in this study. According to Fig. 1, fatigue specimens were manufactured by machining cylindrical bars of 24 mm in diameter and 120 mm in length obtained from investment casting, as per ASTM E606 (Cameron *et al.*, 1996). Then, to make sure there are no surficial or internal defects, all specimens were inspected by the Fluorescent Penetration Inspection (FPI) and X-ray test method.

The next step involved a solution heat treatment at 1205 °C for 2 h and first aging treatment at 1095 °C for 4 h (Rush, 2012). After grit blasting and cleaning the specimens with acetone, an intermediate layer of nickel with a thickness of 1–2 µm was applied on the gauge area of the specimens for decreasing the negative effect of the chromium (available on the composition of the alloy) on the lack of adhesive property of platinum. Then, the gauge area of the specimens was coated with a layer of Pt using an electroplating method. Platinum plating was carried out using an electrolyte solution containing 14–18 ml of type P salt (di-nitro di-amino platinum), 70–90 $g \cdot L^{-1}$ calcium carbonate ($Na_2CO_3$), 40–70 $g \cdot L^{-1}$ sodium acetate ($NaCH_3COO$), and 1L of distilled water at 90 °C under a current density of 0.2-0.4 $A \cdot dm^{-2}$ and electrolyte pH of about 10.5 (Rashidghamat and Shirvani, 2009). In order to achieve a platinum layer with a thickness of 6 µm, the time of 360 min was considered for the plating process. The platinum layer was subjected to heat

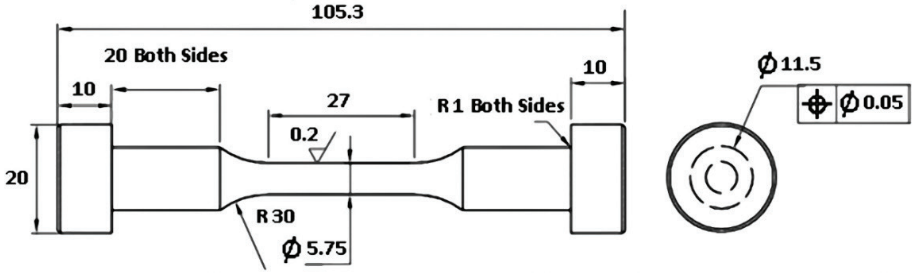


FIGURE 1. Dimensions of the standard fatigue test specimen according to ASTM E606 standard (Cameron *et al.*, 1996).

treatment at 1050 °C for 2 h to enhance cohesion and distribution of the platinum into the substrate, followed by cooling the specimens in a furnace at 400 °C and then air-cooled (Pedraza *et al.*, 2006). The aluminizing process was performed under Low Temperature-High Activity (LTHA), at 750 °C for 4 h followed by post aluminizing for 2 h at 1050 °C, via powder cementation. Composition of the cementation powder used for LTHA condition was selected as $2NH_4Cl$ (Activator) -12Al (Main Agent) -$86Al_2O_3$ (Filler). After the formation of the Pt-Al coating on the surface, an aging treatment was performed at 845 °C for 16 h (Rush, 2012).

Microstructural characterization and fractography studies were conducted using a scanning electron microscope (SEM) Model Zeiss Supra 55 equipped with energy dispersive spectroscopy (EDS) Oxford Model, both prior to performing fatigue test (to ensure the quality of the coating) and after the test (to investigate fracture surfaces) according to ASTM E3 (Brown and Donmez, 2016), ASTM E407 (Walker and Tarn, 1991), and ASTM E112-96 (Vander Voort, 2004) standards. X-ray diffraction analysis was performed using an Inel Equinox 6000 with X'Pert High Score Plus v2.0, Cu K$\alpha$1 with Graphite monochromator, $2\theta$ = 16° to 93°, to determine distributions of different phases across the coating thickness. Micro-hardness testing was carried out normal to the alignment of the Pt-Al coating and the substrate according to ASTM E384 (Grote and Antonsson, 2010) using an automatic Akashi micro-hardness tester equipped with the Clemex software through applying 50 gf. Tensile tests were performed on coated and uncoated specimens at 982 °C using a Universal ATM apparatus equipped with an electrical furnace that could apply temperatures up to 1000 °C ± 1. The tensile tests were performed with a constant strain rate of $1.6\times10^{-4}$ $s^{-1}$, in accordance with ASTM E21 standard procedure (Kuhn and Medlin, 2000). Finally, low cycle fatigue tests were performed on the coated and uncoated specimens at 871 °C and 982 °C according to ASTM E606 standard test method (Cameron *et al.*, 1996), $\Delta\varepsilon_t = 0.8\%$, strain rate of $2\times10^{-3}$ $s^{-1}$, tensile-tensile triangular wave, and $R = \varepsilon_{min}/\varepsilon_{max} = 0$. A servo-hydraulic Instron fatigue test machine equipped with an electrical furnace (1000 °C ± 1) and a high temperature extensometer used to conduct high temperature fatigue tests in strain control mode. It should be mentioned that prior to testing at elevated temperatures, the specimens were allowed to come to thermal equilibrium for 20 min at zero load.

## 3. RESULTS AND DISCUSSION

### 3.1. Microstructural characterization

The microstructures of the substrate (Rene®80) and the coating are shown in Fig. 2. No difference was seen between the microstructure of coated and uncoated substrate.

The microstructure of the Rene®80 Fig. 2a consisted of a $\gamma$-phase matrix, primary, and secondary $\gamma'$. Studies have indicated that there are no changes in the morphology, size and distribution of the $\gamma'$ ($Ni_3(Al,Ti)$) phase (strengthening precipitates) in both coated and uncoated substrates. Hardness of the coated and uncoated substrates was measured as 404 and 408 HV, respectively. The average grain size of the coated and uncoated substrate was found to be 0.4–0.6 mm (measured on a Clemex image analyzer v3.5) according to the ASTM E-112-96 standard (Vander Voort, 2004). Figure 2b shows the cross-sectional microstructure of the coating used in the present study (6 µm Pt/LTHA). The coating exhibited the typical three-layer structure. As shown in this figure, the outer layer contained $\xi$-$PtAl_2$ (bright contrast) and $\beta$-(Ni, Pt)Al. The presence of $\xi$-$PtAl_2$ and $\beta$-(Ni, Pt)Al phases, in this layer, was also confirmed from XRD analysis (Fig. 3). The intermediate layer constituted single-phase $\beta$-(Ni,Pt)Al and final layer named inter-diffusion zone (IDZ, the coating-substrate interface). The thicknesses of the outer layer, the intermediate layer and IDZ were measured 44 ±4, 92 ±7 and 4 ±1 µm, respectively. Hardness in the distance of 15 µm from the surface of the coating was measured 1011 HV, while this value was measured 728 HV in the depth of 125 µm from the coating surface. This high value of hardness shows the brittle nature of Pt-Al coatings.

The concentration plots for Pt, Al and Ni in the coating are shown in Fig. 4. Results of EDS line scan analysis are indicative of internal diffusion of platinum and aluminum and external diffusion of nickel. As shown

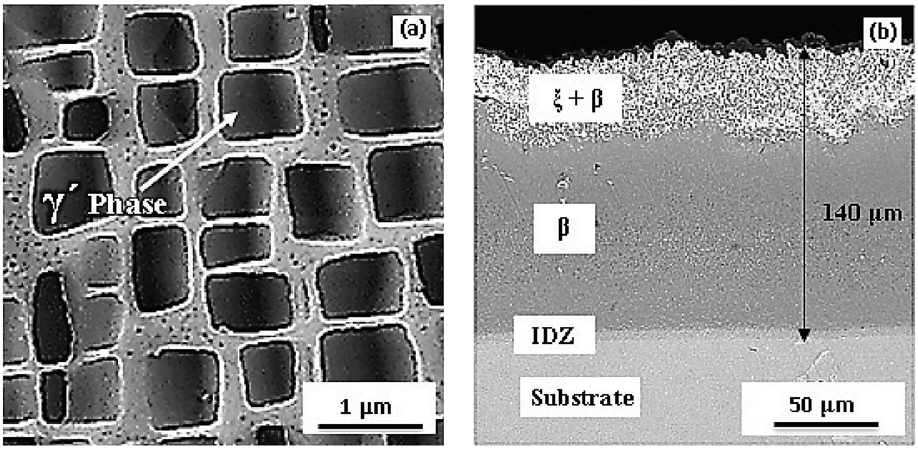


FIGURE 2. SEM images of (a) the γ´ phase of Rene®80 substrate (b) Pt–Al coating in LTHA for platinum layer thicknesses of 6 µm.

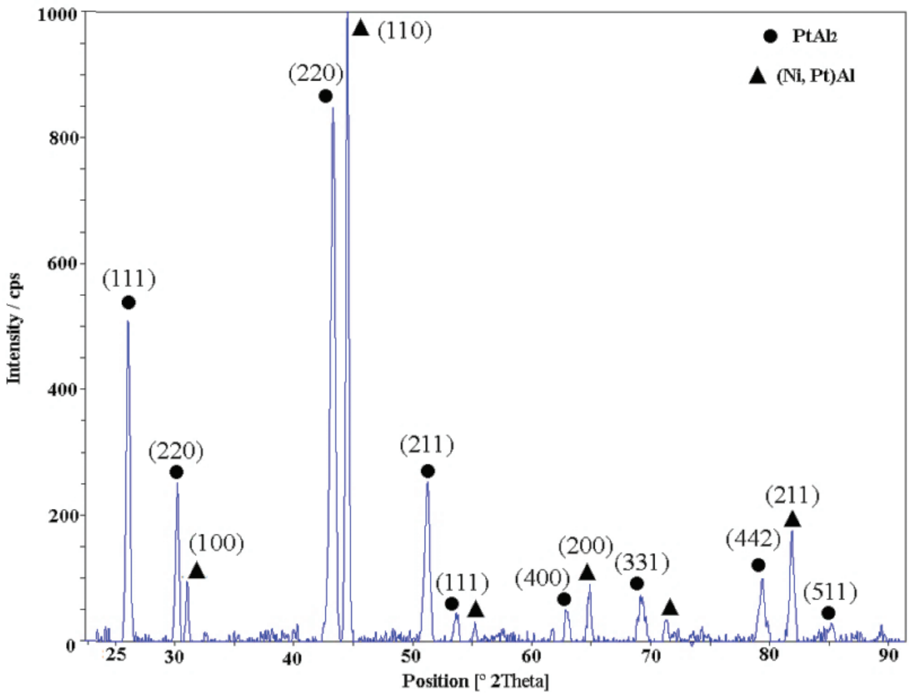


FIGURE 3. Results of XRD analysis on Pt-Al coating used in the present study.

in this figure, the surface Pt concentration is about 40 wt.%. Based on the report by Pedraza *et al.* (2006), at least 28 wt.% of platinum in the surface of Pt-Al coating is necessary to constitute a bi-phase structure.

### 3.2. Low cycle fatigue behavior

#### *3.2.1. Monotonic stress-strain behavior (Tensile Properties)*

The tensile test of superalloy coated and uncoated Rene®80 results and discussions obtained at 871 °C have been reported by us previously (Barjesteh *et al.*, 2019b). The results are shown in Table 1. According to the results, the tensile properties of coated specimens are lower than uncoated specimens. In the present study, tensile test is evaluated on coated and uncoated specimens at 982 °C. The results of the test for this condition are reported in Table 2. It should be mentioned that tensile test at this temperature was performed on two uncoated specimens (after full heat treatment, according to GE-C50TF28 (AMS 5403) (Rush, 2012) and two coated (6 µm Pt/LTHA) specimens. As it can be observed obvious from the Tables 1 and 2, by increasing the

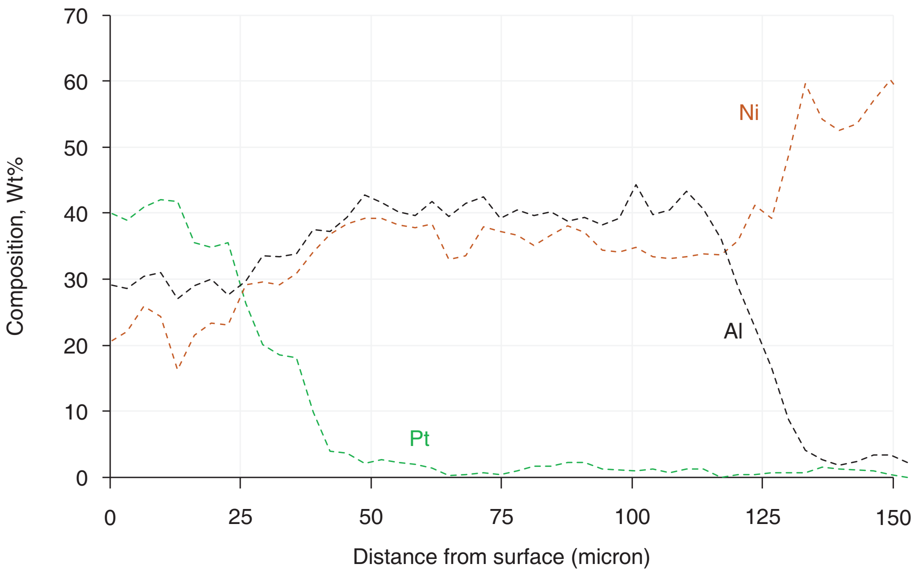


Figure 4. EDS composition profile of Pt, Al and Ni in the used Pt-Al coating.

Table 1. Results of tensile test on coated and uncoated Rene®80 alloy at 871 °C (Barjesteh *et al.*, 2019b)

| **Tensile Properties** | | **UTS (MPa)** | **YS (MPa)** | **El%** | **RA%** |
|---|---|---|---|---|---|
| GE-C50TF28 (AMS5403)/min | | 620 | 415 | --- | 15 |
| Uncoated | Sample 1 | 706 | 595 | 9 | 16.5 |
| | Sample 2 | 696 | 585 | 7 | 15.5 |
| Coated | Sample 1 | 655 | 550 | 7 | 16 |
| | Sample 2 | 651 | 548 | 7 | 16 |

Table 2. Results of tensile test on coated and uncoated Rene®80 alloy at 982 °C

| **Tensile Properties** | | **UTS (MPa)** | **YS (MPa)** | **El%** | **RA%** |
|---|---|---|---|---|---|
| Uncoated | Sample 1 | 355 | 265 | 12 | 20 |
| | Sample 2 | 348 | 258 | 10 | 18 |
| Coated | Sample 1 | 345 | 245 | 12.5 | 26 |
| | Sample 2 | 334 | 234 | 10.5 | 23 |

testing temperature from 871 °C to 982 °C, in both uncoated and coated specimens, ultimate tensile strength (UTS) and yield strength (YS) have been rapidly decreased while ductility (elongation (El%) and reduction of area (RA%)) of uncoated and coated specimen increased. For example, coated specimen showed 55.4% lower YS at 982 °C compared to 871 °C while the elongation of coated specimen at 982 °C was about 64.2% higher than this property at 871 °C. The strength of Pt-Al coatings is lower than that of the substrate alloy on which they are deposited (Alam *et al.*, 2011). For example, yield and ultimate strengths of Pt–Al coatings were equal to 200 and 300 MPa at a temperature range of 800–900 °C, respectively, which was lower than the yield strength (595 MPa) and ultimate strength (706 MPa) of the Rene®80 alloy (Table 1) at 871 °C. Different fracture stress will be made with this huge difference between the coating and substrate strengths that give rise to the formation of some cracks on the coating during the usage of tensile load. Therefore, it can be expected that the presence of the coating would cause some degree of weakening of the base alloy.

Fractographic studies of the uncoated and coated (6 μm Pt/LTHA) tensile specimens at 871 °C in the previous investigation (Barjesteh *et al.*, 2019b) exhibited that the fracture mechanism was a mixed mode of ductile and brittle fracture. The results of the previous study also showed that most of the cracks nucleate from grain boundaries and propagate along them in the uncoated specimens, while cracks initiated from the coating surface in the coated specimens. Figure 5 shows the SEM images of uncoated and coated specimens failed during a tensile test at 982 °C. As it can be observed from Fig. 5a, at higher temperature, not only grain boundaries and thick oxide layer are the suitable locations for crack nucleation, in the uncoated specimens, but also internal voids are other appropriate sites. With increase in test temperature, more dimples with the large size could be observed in the uncoated specimens (Fig. 5b). According to Fig. 5c, profuse large dimple formation also occurred in the coated specimens, at 982 °C. SEM image of the fracture surface (longitudinal section) at 982 °C of coated specimens is provided in Fig. 5d.

Extensive void formation and ductile failure were seen across the coating thickness. The fracture surface features of the superalloy substrate at high temperatures were similar to those of uncoated specimens. To study the crack behavior in coated specimens, the longitudinal section of these specimens after the tensile test was examined. According to Fig. 5e, the crack remained in the coating thickness range and no penetration of cracks into the substrate has been observed. Other studies (Parlikar *et al.,* 2017) showed a decrease in the extent of crack penetration with the increase in test temperature. However, it is known that these cracks decrease the load bearing cross-section area of the substrate and cause a decrease in the strength of the substrate alloy. As mentioned previously, large dimples have been observed in the cross section of coated specimens, this was because the test temperature (982 °C was well above the DBTT of the coating. Comparison of obtained results with the previous investigation (Barjesteh *et al.*, 2019b) showed that the extent of the ductile fracture region was much more at 982 °C.

### *3.2.2. Cyclic stress-strain behavior of uncoated specimens*

Results of fatigue test on the uncoated Rene®80 specimens at 871 °C and total strain range of 0.8% have been reported by us in the previous study (Barjesteh *et al.*, 2019a). The results of the previous study are shown in Table 3. Low cycle fatigue test of uncoated Rene®80 at 982 °C, also performed in the present study and the results are shown in Table 4, where $\Delta\varepsilon_t$ is total strain amplitude, $\sigma_{max}$ is maximum cyclic stress, $\sigma_{min}$ is minimum cyclic stress, $N_i$ is the number of cycles by which the first drop in the alloy properties is observed (crack nucleation), and $N_f$ is the number of cycles to fracture.

As is seen from Tables 3 and 4, the low cycle fatigue life of the uncoated Rene®80 decreases with increasing test temperature from 871 °C to 982 °C. The results indicated that during the test at 982 °C, specimens showed 46.6% - 54.6% lower fatigue life ($N_f$) compared to the specimens were tested at 871 °C. An increase in temperature led to a decreasing of the strength of γ′ phase and acceleration of an oxidation process so resulting in microstructural deterioration of the alloy (Zhang *et al.,* 2019). The diffusion of Al into the surface as a result of oxidation at high temperature led to an increase in the area of γ′ depleted zones near the surface where initiation and nucleation of the cracks easily start from them. On the other hand, the oxide layer is more brittle than substrate, and therefore, it is an excellent site for crack formation. Rapid and frequent formation of the oxidation layer on the crack tips has an effect on the crack growth rate. This oxide layer is much more brittle than the surrounding alloy and easy to break. In the next stage, following the breakage of the oxidation layer upon the application of cyclic stress, the alloy is exposed to air and hence re-oxidized, smoothing the way for further crack growth until the final failure.

Results of low cycle fatigue test of Rene®80 uncoated specimens at temperatures of 871 °C and 982 °C, in the form of strain vs. stress hysteresis loops are shown in Fig. 6. The hysteresis loops illustrate variations in resistance behavior of the materials against deformation under cyclic loading. Alloys may show cyclically harden, cyclically soften or a mixed behavior depending on their internal resistance to the deformation. This behavior may result from the nature and stability of the dislocation substructure of the materials (Stephens *et al.*, 1980). As can be seen from the diagrams plotted in Fig. 6, the maximum stress obtained decreases with each cycle of strain in the low cycle fatigue test of Rene®80 at both temperatures of 871 °C and 982 °C and at R = 0. This is known as cyclic softening. Generally in the alloy, if *UTS / YS* < 1.2 (where *UTS* is ultimate strength and *YS* is yield strength), the alloy will show cyclic softening behavior and if *UTS /YS* > 1.4, the alloy will exhibit cyclic hardening behavior (Bannantine *et al.,* 1990). Tensile test results (Tables 1 and 2) show that the condition of *UTS / YS* < 1.2 is true for uncoated specimens at both temperatures of 871 °C and 982 °C. As is evident from Fig. 6a and Fig. 6b, the tension and compressive stress required to enforce the strain decrease with the increasing number of cycles.

The maximum resultant stress at the first cycle of specimen which was tested at 982 °C is lower than that of the specimen one at 871 °C. At the first cycle, initially, slip systems become active in the perpendicular direction to the cyclic stresses, and

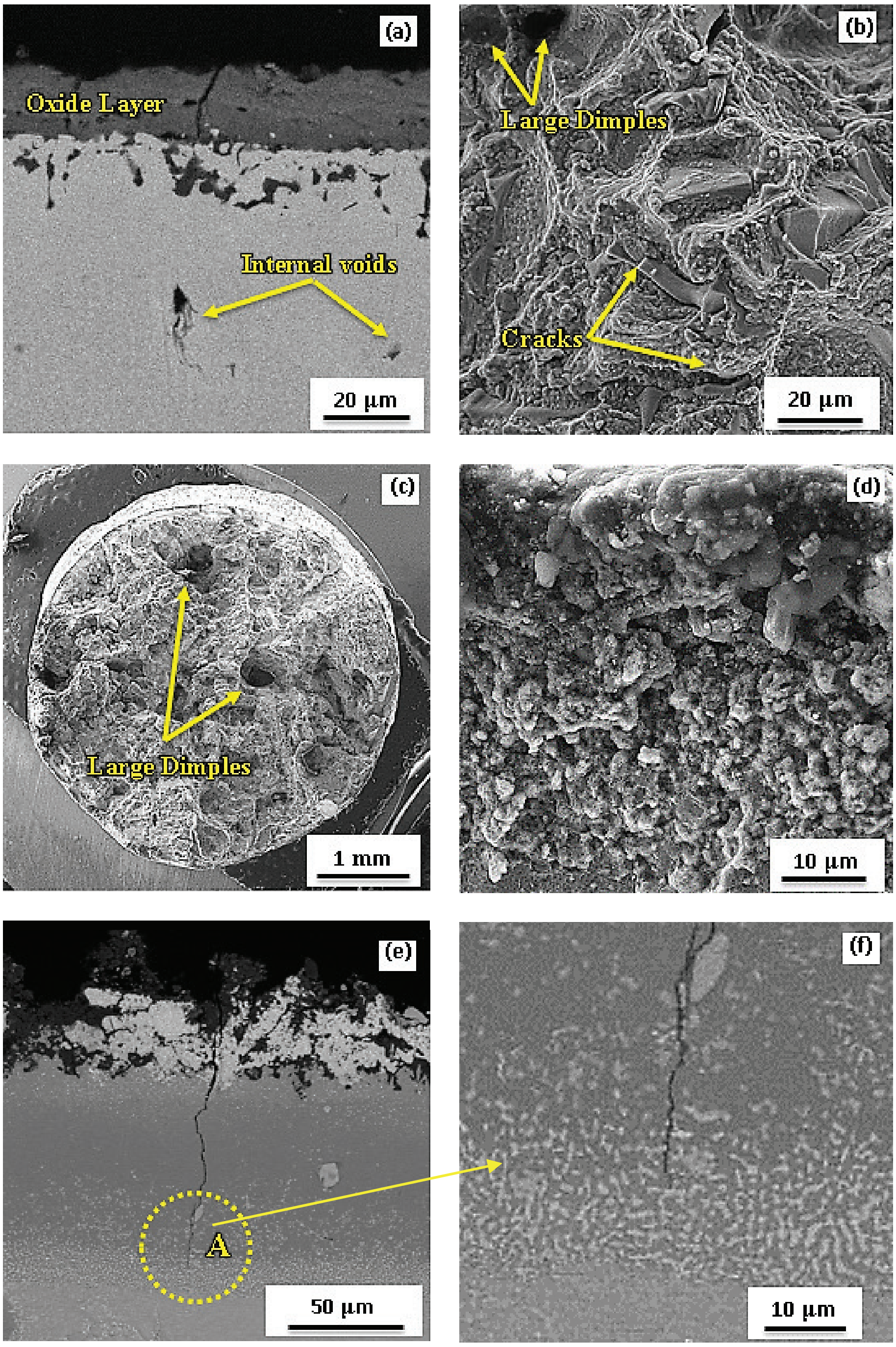


FIGURE 5. SEM images of tensile fracture surface features at 982 °C (a) cracks initiated from oxide layer and internal voids of uncoated specimens, (b) Large dimples formed in the uncoated specimens, (c) Dimple fracture in the coated specimens, (d) extensive void formation and ductile failure in the coated specimens, (e) Crack remained in the coating and (f) Region of A at higher magnification.

dislocations are concentrated in the γ matrix phase due to its lower strength compared to the precipitation γ′ phase. As the number of cycle increases, the deformations become homogeneous and more slip systems become active, and as a result, the density of dislocations is increased. Upon dislocation-dislocation interactions and the cutting of γ′ by dislocations, the strength of the superalloy decreases and the specimen is failed at the $N_f$ cycle (Rahmani and Nategh, 2008b). On the other hand, by increasing the temperature, the mobility of atoms increases and diffusion-controlled mechanisms become active, dislocation mobility increases, slip becomes easier, new slip systems become available, and finally, the fracture of specimen can occur sooner (Campbell, 2012).

Figure 7 shows variations of the maximum and minimum stresses and the stress range ($\Delta\sigma = \sigma_{max} - \sigma_{min}$) as functions of time for uncoated specimens at two temperatures of 871 °C and 982 °C. As is evident from the Fig. 7, the rate of change of the stress reduces and the stress magnitude reaches a stable level which is named steady state condition. This condition remains stable for the rest of the fatigue life until the detection of the first fatigue crack. With the creation of the first crack at time $t_i$ (the $N_i$ cycle), the stress level suddenly drops and the specimen fails after a limited number of cycles at time $t_f$ (the $N_f$ cycle). As can be concluded from this figure, the tensile stress, decreasing at 982 °C is greater than at 871 °C, also test duration of uncoated specimen at 871 °C was about 60 min, while this time was reduced almost 46% for the same specimen at 982 °C.

Figure 8 shows the fracture surface of the uncoated specimen of the alloy Rene®80 after low cycle fatigue failure at 871 °C and 982 °C, at the total strain range of 0.8%. Comparing Fig. 8a with

TABLE 3. Results of low-cycle fatigue test on uncoated Rene®80 specimens ($\Delta\varepsilon_t$ (%) =0.8, R =0, $\dot{\varepsilon} = 2 \times 10^{-3}\ s^{-1}$) (Barjesteh *et al.*, 2019a)

| **T (°C)** | **$\sigma_{max}$ (MPa)** | **$\sigma_{min}$ (MPa)** | **$N_i$** | **$N_f$** |
|---|---|---|---|---|
| **871** | 742.5 | -532 | 422 | 487 |
| | 757 | -550.4 | 425 | 474 |

TABLE 4. Results of low-cycle fatigue test on uncoated Rene®80 specimens ($\Delta\varepsilon_t$ (%) = 0.8, R = 0, $\dot{\varepsilon} = 2\times10^{-3}\ s^{-1}$)

| **T (°C)** | **$\sigma_{max}$ (MPa)** | **$\sigma_{min}$ (MPa)** | **$N_i$** | **$N_f$** |
|---|---|---|---|---|
| **982** | 406 | -391 | 155 | 221 |
| | 412 | -369 | 190 | 253 |

Fig. 8b shows that the micro-void numbers in the superalloy substrate at higher temperature (982 °C) are more than those of lower temperature (871 °C). The presence of these micro-voids showed a ductile fracture. Also cleavage fracture (brittle fracture) can be observed in the fracture surface of both specimens. However, in comparison with specimen which was tested at 982 °C, the morphology of cleavage fracture could be seen in the larger region at 871 °C. Therefore, it could be said that the fracture mechanism was a mixed mode of ductile and brittle fracture for both temperatures, although fracture at 871 °C was more brittle. In Fig. 8c dimples at 982 °C were shown at high magnification (with increase in test temperature, profuse dimple formation occurred). Fig. 8d shows a longitudinal view of the fracture surface of the uncoated specimen, at 982 °C. The cracks were seen to be nucleated on the alloy surface under the effects of cyclic loads. As observed, the crack is nucleated on the alloy surface from the thick oxidized layer and grew in the normal direction to the loading axis. Performing tests at elevated temperature results in the surface oxidation of the uncoated alloy, and these points provide suitable sites for fatigue crack nucleation. As mentioned before, because of the diffusion of Al into the surface due to oxidation, γ′ phase will be poor in this element. Due to the depletion of the near-surface area from γ′, the alloy strength decreases, providing a basis for micro-crack nucleation. Also, more studies (Gopinath *et al.*, 2009; Zhang *et al.*, 2018) show that the fatigue crack nucleation has taken place beneath the surface where there are some internal defects, such as internal voids, inclusions and debris.

The typical observation of γ′ microstructure after LCF test at temperatures of 871 °C and 982 °C, is given in Fig. 9. As shown in this figure, increasing the temperature test from 871 °C to 982 °C, has no a significant effect on the γ′ morphology of the substrate, while the shape of this phase has remained almost in its cubic morphology.

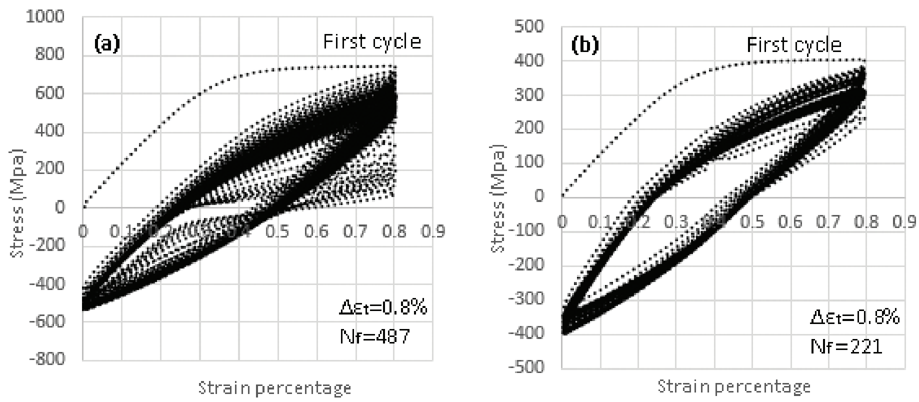


FIGURE 6. Stress-strain hysteresis loop at Δεt= 0.8% for uncoated specimens at (a) 871 °C (Barjesteh *et al.*, 2019a) and (b) 982 °C.

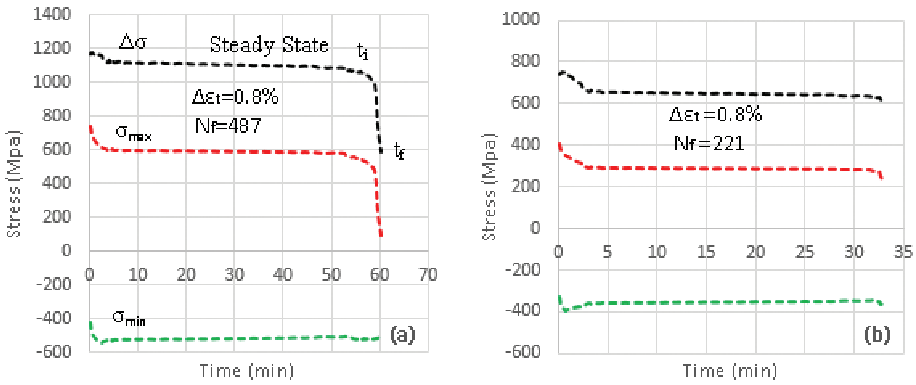


FIGURE 7. Maximum and minimum stresses *vs* time at $\Delta\varepsilon_t = 0.8\%$ for uncoated specimens at (a) 871 °C (Barjesteh *et al.*, 2019a) and (b) 982 °C.

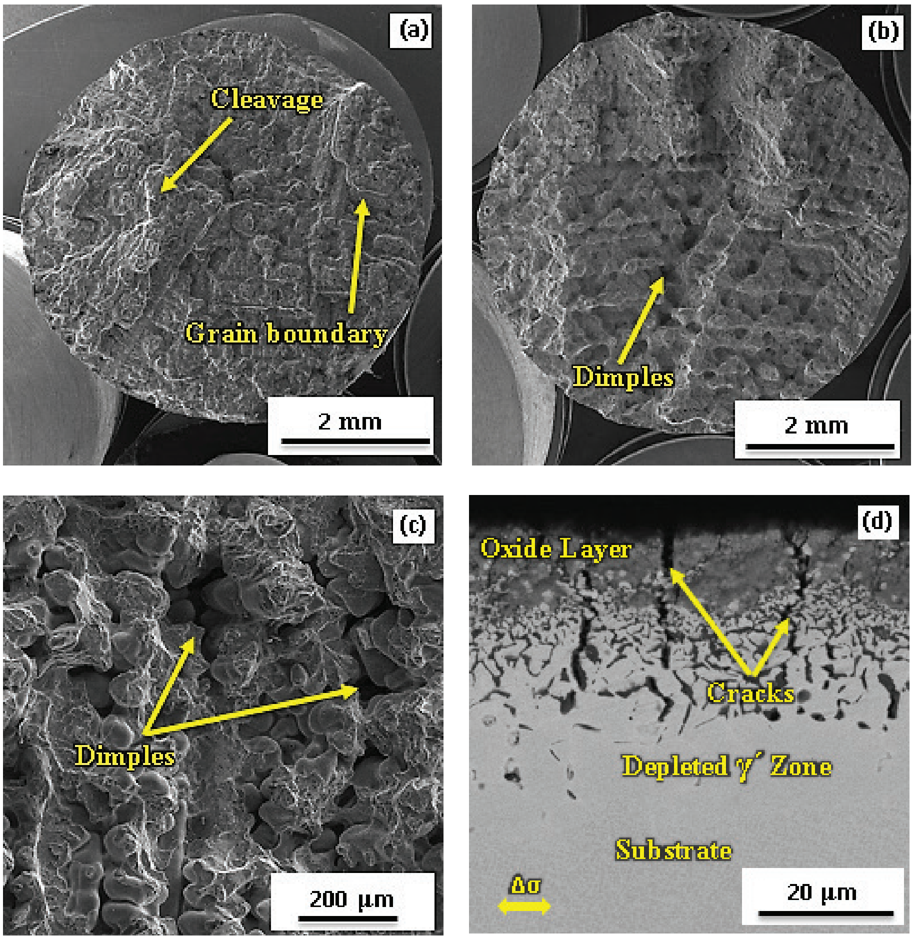


FIGURE 8. SEM images of LCF fracture surface of uncoated specimen at $\Delta\varepsilon_t = 0.8\%$: (a) cleavage and small dimples at 871 °C, (b) large dimples at 982 °C, (c) Dimples at 982 °C at higher magnification, and (d) Cracks initiated from oxide layer at 982 °C.

### *3.2.3. Cyclic stress-strain behavior of coated specimens*

The results of the low cycle fatigue tests on the coated specimens (6 µm Pt-LTHA) at 871 °C and 982 °C are presented in Table 5. It should be mentioned that LCF test at each temperature was performed on two coated specimens.

Experimental results show that, in coated specimens, while the total strain is equal to 0.8%, the presence of coating at 871 °C decreases the fatigue life, but in temperature of 982 °C fatigue lifetime of

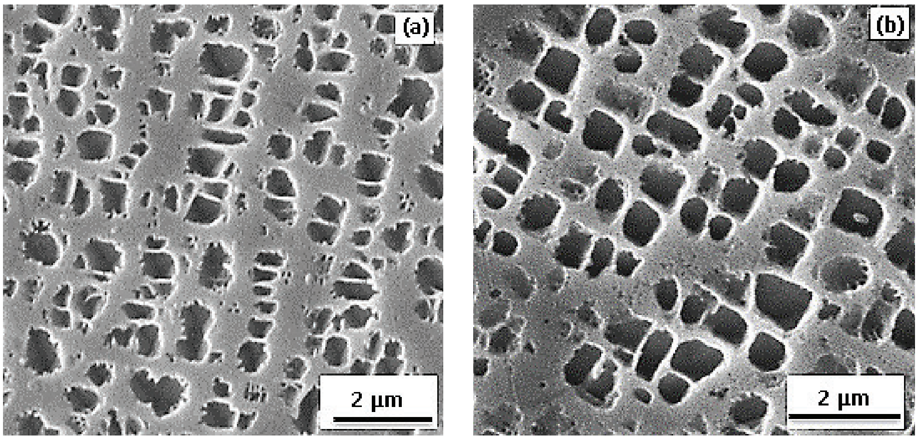


FIGURE 9. SEM images of γ′ morphology after LCF test at $\Delta\varepsilon_t$= 0.8%: (a) 871 °C and (b) 982 °C.

TABLE 5. Results of low-cycle fatigue test on coated Rene®80 specimens at 871 °C and 982 °C ($\Delta\varepsilon t$ (%) = 0.8, R = 0, $\dot{\varepsilon}$ = $2\times10^{-3}$ $s^{-1}$)

| T (°C) | $\sigma_{max}$ (MPa) | $\sigma_{min}$ (MPa) | $N_i$ | $N_f$ |
|---|---|---|---|---|
| **871** | 791 | -548 | 386 | 416 |
| | 798 | -554 | 382 | 410 |
| **982** | 400 | -380 | 178 | 245 |
| | 418 | -345 | 192 | 280 |

the coated specimens is more than that of uncoated specimens at the same total strain. At this temperature, the coated specimen tolerated 245–280 cycles to fail, indicating about 10% increase in the number of tolerated cycles, as compared to the uncoated specimen.

In Figs. 10 and 11 hysteresis loops and variations of stress with time for coated specimens at 871 °C and 982 °C are shown. As is evident from the figures, the fatigue behavior of the coated specimens resembled those of the uncoated specimen, i.e., showing a cyclic softening behavior.

It seems that, by increasing the testing temperature, the more consistency between the coating and the substrate is detected. One of the reasons supporting the increment of fatigue strength in coated specimen at 982 °C, compared to uncoated specimen, is the high ductility of this specimen. As is seen from the tensile test results (Tables 1 and 2), the coated specimen at 982 °C showed the best ductility. On the other hand, the presence of the Pt-Al coating prevents oxidation damage of the substrate alloy at elevated temperatures (Chen *et al.*, 2015). This phenomenon plays an effective role in the limitation of the crack nucleation from the thick oxide layer which is formed on the surface of uncoated specimens. Therefore, it is expected to have a better fatigue life in coated specimen when working temperature is well above the DBTT of the coating.

Figure 12 shows the surface of coated specimen after fracture at temperatures of 871 °C and 982 °C under cyclic loading ($\Delta\varepsilon_t$ = 0.8%).

It should be mentioned that, no difference was observed between the coated and the uncoated substrate at these temperatures, i.e., the morphology of γ′ was stable and similar to Fig. 9. A mixed mode of ductile and brittle failure was investigated at both temperatures (Fig. 12a and 12b). As seen from Fig. 12c, the cracks nucleation started from the surface of the coating at 871 °C and grew in the normal direction to the loading axis and confined to within the coating and did not penetrate the substrate. It seems that at this temperature and strain level the coating is brittle enough to create a suitable site for crack nucleation. The single phase intermediate layer of β-(Ni, Pt)Al played an important role in strength properties of the coatings and also has a marked effect on DBTT. The reasons for the brittleness of β-(Ni, Pt)Al coating (bcc structure) are the insufficient number of slip systems and grain boundary weakness (Rao, 2003). The creation of cracks in the coating causes a continuously diminishing load bearing cross-section of the coated specimen and hence the fatigue life will be declined in comparison to of uncoated specimens.

The presence of the cracks in the coating and no penetration of that to the substrate, show that, the LCF test was performed near DBTT. DBTT is related to the capability of the β-(Ni, Pt)Al phase to plastically deform under load and highly depends on chemical composition of coatings (Bose, 2007). As can be seen from Fig. 4, the weight percentage of aluminum in the coating composition was measured about 40%. This value is high and plays an effective role in the increasing of the DBTT. On the other hand, by adding the platinum in Ni-Al coating, the DBTT of the coating increases due to the improved solid solution hardening and the promotion of ductile-to-brittle phase transformations, e.g. γ→ γ’

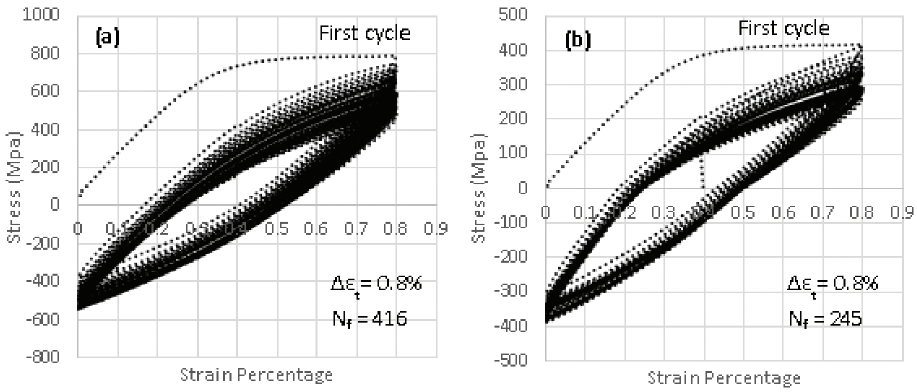


FIGURE 10. Stress-strain hysteresis loop at Δεt= 0.8% for coated specimens at (a) 871 °C and (b) 982 °C.

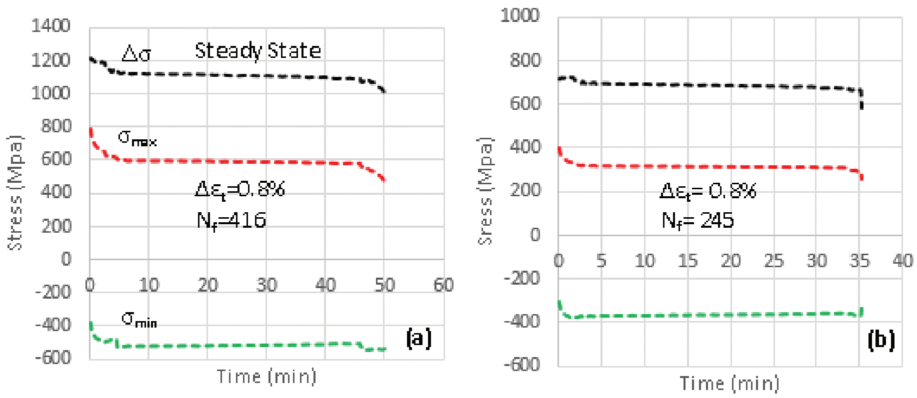


FIGURE 11. Maximum and minimum stresses *vs* time at $\Delta\varepsilon_t$ = 0.8% for coated specimens at (a) 871 °C and (b) 982 °C.

(($Ni_3Al$,Ti) (DBTT: 730–900 °C)) → β ((Ni,Pt)Al) (DBTT: 868–1060 °C)). DBTT of the $PtAl_2$ phase is also reported 870–1070 °C (Tamarin, 2002).

Figure 12d shows longitudinal section of the coated specimens tested at 982 °C. As can be observed from this figure, no cracks have been detected in the Pt-Al coating at this temperature. As shown in Fig. 12e, cracks initiated from internal voids and carbide interfaces at 982 °C. Result of EDS analysis at point A (Fig. 12b) has been shown in Fig. 12f. The presence of TiC as internal carbides within the dimples was confirmed by this analysis. The existence of carbide particles inside the dimples is also reported in the other research (Parlikar *et al.*, 2017). No presence of the cracks in the Pt-Al coatings at 982 °C can be coupled to the good ductility over the DBTT. In related research (Yuan, 2013), it was mentioned that, above DBTT dislocations within the alloy are able to overcome obstacles to produce more plastic deformation. In the research performed by Rahmani and融 Nategh (Rahmani and Nategh, 2008b), the effect of plain-aluminide coating (CODEP-B) on low cycle fatigue properties of the Rene®80 alloy was considered, and the results indicated that at the condition of T= 871 °C and Δεt = 0.8%, applying the coating CODEP-B on this superalloy increases LCF life. Comparing their conclusions with present results shows that Pt-Al coating on nickel-base superalloys exhibits higher DBTT than that of plain aluminides, while at T= 871 °C and Δεt = 0.8%, applying the Pt-Al coating decreases the fatigue life of Rene®80. On the other side, by increasing the testing temperature from 871 °C to 982 °C, the LCF life of coated specimen will be improved as compared to the uncoated one tested at 982 °C. The current results indicate that the application of Pt-Al coating (6 µm Pt-LTHA) seems to have a beneficial effect on the LCF of Rene®80 when the experimental temperature is much higher than the DBTT.

## 4. CONCLUSIONS

- The results of this study showed that the tensile strength (UTS and YS) of superalloy Rene®80 decreased at temperatures of 871 °C and 982 °C after applying a Pt-Al coating (6 µm Pt-LTHA), but ductility (E.L% + R.A%) of coated Rene®80 increased at 982 °C. A combination of ductile and brittle fracture modes observed from the

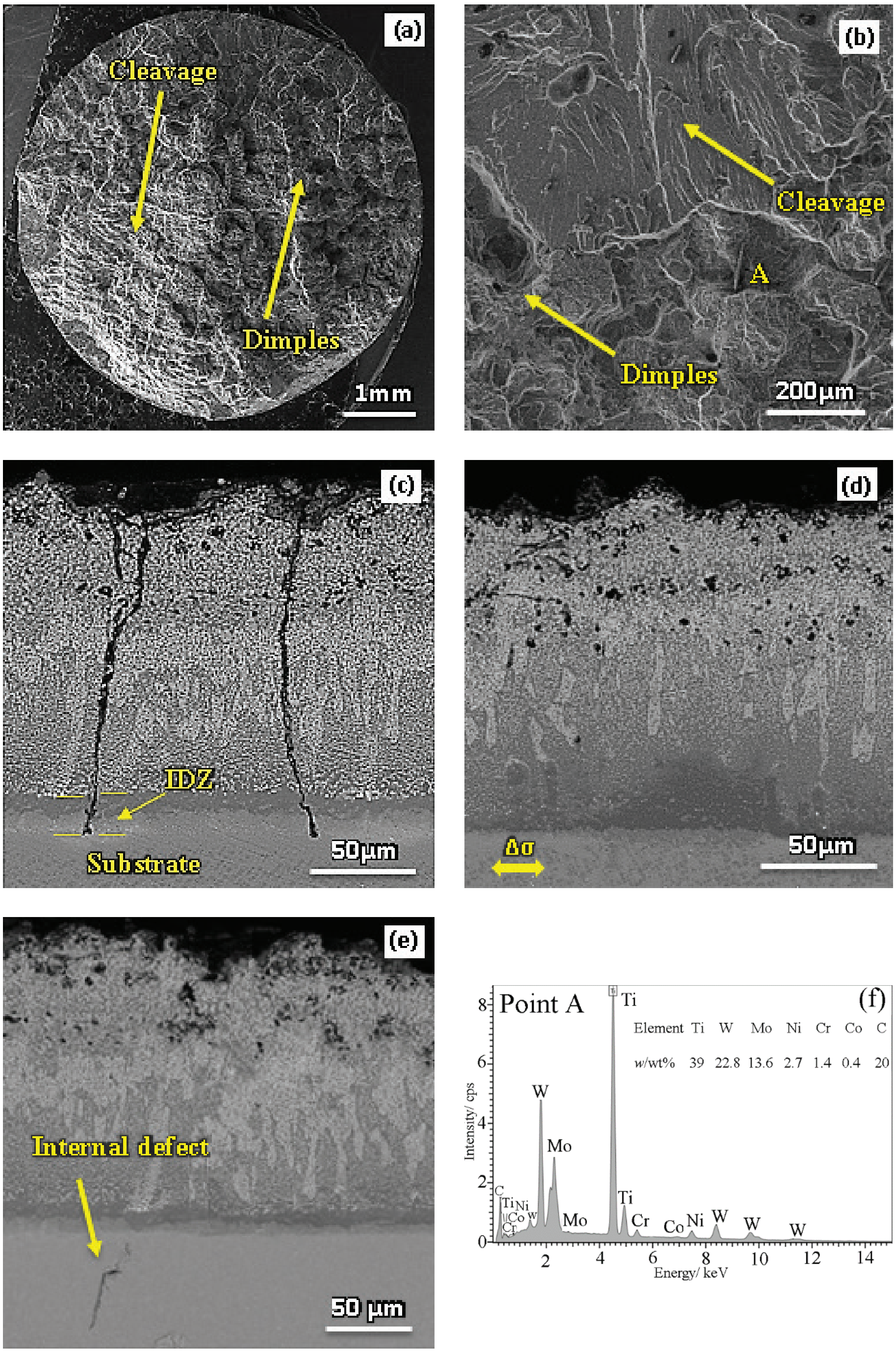


FIGURE 12. SEM images of the failed fatigue specimens at Δεt = 0.8%, R=0: (a) and (c) at 871 °C, (b) and (d) at 982 °C, (e) crack initiated from internal defects at 982 °C, and (f) EDS analysis at Point A of Fig. 12b.

cross-section (longitudinal section) of the failed tensile specimens. The ductile region (large dimples) was seen much more on the fracture surface of a specimen which was tested at 982 °C. This further accepted that the test temperature was above DBTT.

- Low cycle fatigue life was reduced in the coated specimens as compared to the uncoated one at 871 °C, while the coated specimens showed 10% more fatigue life compared to the uncoated specimen at 982 °C. The reasons for that relate to good ductility of the coated Rene®80 at 982 °C (above DBTT) and improvement of the oxidation resistance of coated specimens.
- Fracture surface analysis of failed LCF specimens showed a mixed mode of ductile and

brittle failure under cyclic loading in both uncoated and coated specimens.

- Crack behavior investigation showed that at both temperatures, crack initiated from thick oxide layer in the uncoated specimen, while in the coated specimen crack started from coating at 871 °C and stopped in the IDZ. At 982 °C, no cracks were detected in the coating and crack initiated from internal voids and internal defects of the substrate.

## REFERENCES


Alam, M.Z., Chatterjee, D., Kamat, S.V., Jayaram,V., Das, D.K. (2010). Evaluation of ductile-brittle transition temperature (DBTT) of aluminide bond coats by micro-tensile test methods. *Mater. Sci. Eng. A* 527 (26), 7147–7150. https://doi.org/10.1016/j.msea.2010.07.059.

Alam, M.Z., Srivathsa, B., Kamat, S.V., Jayaram, V., Das, D.K. (2011). Study of brittle-to-ductile-transition in Pt-aluminide bond coat using micro-tensile testing method. *Trans. Indian Inst. Met.* 64 (57), 57–61. https://doi.org/10.1007/s12666-011-0011-y.

Bannantine, J.A., Comer, J.J., Handrock, J.L. (1990). *Fundamentals of Metal Fatigue Analysis*. Printice Hall.

Barjesteh, M.M., Zangeneh-Madar, K., Abbasi, S.M., Shirvani, K. (2019a). The effect of platinum-aluminide coating features on high temperature fatigue life of nickel-based superalloy Rene®80. *J. Min. Metall. B* 55 (2), 235–251. https://doi.org/10.2298/JMMB181214029B.

Barjesteh, M.M., Abbasi, S.M., Zangeneh-Madar, K., Shirvani, K. (2019b). Correlation between platinum–aluminide coating features and tensile behavior of nickel-based superalloy Rene@80. *Rare Met*. https://doi.org/10.1007/s12598-019-01293-4.

Bose, S. (2007). *High Temperature Coating.* 1st Edition, Butterworth-Heinemann.

Brown, C.U., Donmez, A. (2016). Microstructure Analysis for Additive Manufacturing: A Review of Existing Standards. National Institute of Standards and Technology, U.S. Department of Commerce. https://doi.org/10.6028/nist.ams.100–3.

Cameron, D.W., Allegany, N.Y., Hoeppner, D.W. (1996). *Fatigue and Fracture, Fatigue Properties in Engineering*. ASM Handbook, Vol. 19, ASM International, pp. 36–56.

Campbell, F.C. (2012). Fatigue and fracture, Understanding the basics. ASM International.

Chen, Y., Zhao, X., Bai, M., Chandio, A., Wu, R., Xiao, P. (2015). Effect of platinum addition on oxidation behaviour of γ/γ′ nickel aluminide. *Acta Mater.* 86, 319–330. https://doi.org/10.1016/j.actamat.2014.12.023.

Gopinath, K., Gogia, A.K., Kamat, S.V., Balamuralikrishnan, R., Ramamurty, U. (2009). Low cycle fatigue behaviour of a low interstitial Ni-base superalloy. *Acta Mater.* 57 (12), 3450–3459. https://doi.org/10.1016/j.actamat.2009.03.046.

Grote, K.H., Antonsson, E.K. (2010). *Springer handbook of mechanical engineering*. *Part B, Applications in mechanical engineering*. Springer Sci, USA. p.121.

Krishna, G.R., Das, D.K., Singh, V., Joshi, S.V. (1998). Role of Pt content in the microstructural development and oxidation performance of Pt aluminide coatings produced using a high-activity aluminizing process. *Mater. Sci. Eng. A* 251 (1–2), 40–47. https://doi.org/10.1016/S0921-5093(98)00655-8.

Kuhn, H., Medlin, D. (2000). *ASM Handbook Vol. 8*, *Mechanical Testing and Evaluation.* Materials Park, Ohio, USA, pp. 152–163.

Parlikar, C., Alam, M.Z., Chatterjee, D., Das, D.K. (2017). Thickness apropos stoichiometry in Pt-aluminide (PtAl) coating: Implications on the tensile properties of a directionally solidified Ni-base superalloy. *Mater. Sci. Eng. A* 682, 518–526. https://doi.org/10.1016/j.msea.2016.11.074.

Pedraza, F., Kennedy, A.D., Kopecek, J., Moretto, P. (2006). Investigation of the microstructure of platinum-modified aluminide coatings. *Surf. Coat. Tech.* 200 (12–13), 4032–4039. https://doi.org/10.1016/j.surfcoat.2004.12.019.

Rahmani, K., Nategh, S. (2008a). Influence of aluminide diffusion coating on the tensile properties of the Ni-base superalloy René 80. *Surf. Coat. Tech.* 202 (8), 1385–1391. https://doi.org/10.1016/j.surfcoat.2007.06.041.

Rahmani, K., Nategh, S. (2008b). Low cycle fatigue mechanism of René 80 at high temperature–high strain. *Mater. Sci. Eng. A* 494 (1–2), 385–390. https://doi.org/10.1016/j.msea.2008.04.067.

Rao, K.B.S. (2003). High temperature fatigue behaviour of intermetallics. *Sadhana* 28, 695–708. https://doi.org/10.1007/BF02706454.

Rashidghamat, A., Shirvani, K. (2009). *Electrodeposition of platinum on nickel-base superalloy Rene-80*. In: EFC Workshop on Solutions for High Temperature Corrosion Protection in Energy Conversion System, Frankfurt, Germany.

Rush, M.T. (2012). Development of weld repair methods for Rene 80 nickel based superalloy. Ph.D thesis, Cranfield university, School of Applied Sciences.

Safari, J., Nategh, S. (2006). On the heat treatment of Rene-80 nickel-base superalloy. *J. Mater. Process Tech.* 176 (1–3), 240–250. https://doi.org/10.1016/j.jmatprotec.2006.03.165.

Stephens, I., Fatemi, A., Stephens, R.R., Fuchs, H.O. (1980). *Metal Fatigue in Engineering*. A Wiley-interscience publication, John Wiley & Sons, 2nd Edition.

Tamarin, Y. (2002). *Protective coatings for turbine blades*. ASM International.

Vander Voort, G.F. (2004). *ASM Handbook Vol. 9, Metallography and Microstructures.* Materials Park, Ohio, USA, pp. 403–427.

Vogel, D., Newman, L., Deb, P., Boone, D.H. (1987). Ductile-to-brittle transition temperature behavior of platinum-modified coatings. *Mater. Sci. Eng. A* 88, 227–231. https://doi.org/10.1016/0025-5416(87)90089-9.

Walker, P., Tarn, W.H. (1991). *CRC Handbook of metal etchants*. CRC Press LLC.

Yuan, K. (2013). Thermal and Mechanical Behaviors of High Temperature Coatings. Ph.D thesis, Linkoping University.

Zhang, X., Gao, H., Wen, Z., Zhang, H., Yue, Z. (2018). Low Cycle Fatigue Failure Analysis of a Ni-Based Single Crystal Superalloys at 850 °C. *Adv. Eng. Mater.* 21 (2), 1–11. https://doi.org/10.1002/adem.201800647.

Zhang, L., Zhao, L.G., Roy, A., Silberschmidt, V.V., McColvin, G. (2019). Low-cycle fatigue of single crystal nickel-based superalloy – mechanical testing and TEM characterization. *Mater. Sci. Eng. A* 744, 538–547. https://doi.org/10.1016/j.msea.2018.12.084.